ELSEVIER

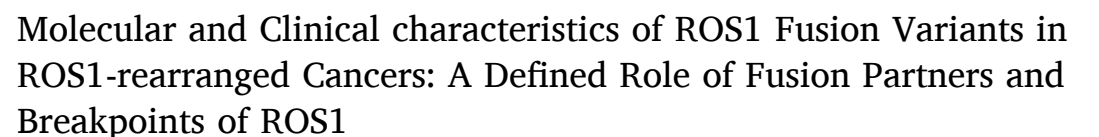
Contents lists available at ScienceDirect

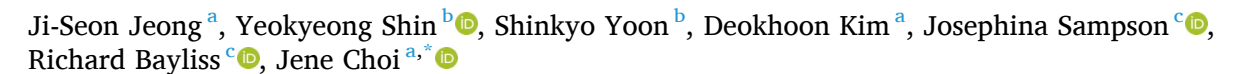
# European Journal of Cancer

journal homepage: www.ejcancer.com



# Original research





- <sup>a</sup> Departments of Pathology, University of Ulsan College of Medicine, Asan Medical Center, Seoul, South Korea
- <sup>b</sup> Department of Oncology, University of Ulsan College of Medicine, Asan Medical Center, Seoul, Korea

#### ARTICLE INFO

#### Keywords: ROS1 fusion Breakpoint Fusion partner Non-small cell lung cancer ROS1-TKI

## ABSTRACT

*Introduction:* ROS1-targeted tyrosine kinase inhibitors (TKIs) are the standard treatment for *ROS1*-rearranged cancers. We here investigated the therapeutic significance of multiple fusion partners and variable *ROS1* genomic breakpoints

*Methods*: We retrieved 81 *ROS1*-rearranged cases from a clinical DNA-based next generation sequencing cohort and performed comprehensive analyses, including reverse transcription-polymerase chain reaction, RNA sequencing and immunohistochemistry staining. The obtained data were correlated with the clinical responses to ROS1-TKIs.

Results: ROS1 fusions with canonical and  $\sim$ 20 rare fusion partners were identified. ROS1 breaks occurred at rare 12 exon/intron regions together with major breakpoints. High ROS1 expression correlated significantly with major breakpoints and canonical partners and low expression associated with rare breakpoints and non-canonical partners (P < 0.001). Cases with an intron 32 ROS1 breakpoint involved exclusion of exon 33 to generate an in-frame fusion, and canonical fusion partners showed a strong preference for an intron 33 to intron 32 breakpoint (P < 0.001). Significantly better progression-free survival rates (PFSR) were observed among first-line TKI-treated NSCLC patients with ROS1 breakpoints in introns 33 and 34, compared with intron 32 and rare locations (80 %, 33.3 %, and 0 %, respectively; P < 0.001). Patients with at least one major breakpoint or canonical partner also showed significantly better PFSR compared to those with both rare partners and non-major breakpoints (50.4 % vs 0 %, P < 0.001).

*Conclusions*: Canonical fusion partners with introns 33 and 34 of *ROS1* may be the most optimal predictors for ROS1-TKI benefit. Precise characterization of the variants in terms of *ROS1* breakpoints could be important for patient stratification in ROS1-rearranged cancers.

# 1. Introduction

*ROS1* rearrangements occur in 1-2 % of non-small cell lung cancer (NSCLC) patients globally and 2-3 % among East Asian populations [1-4]. The advent of ROS1-targeted tyrosine kinase inhibitors (TKI), such as crizotinib, has significantly improved patient outcomes [5,6]. An

*EML4-ALK* rearrangement, the most common translocation in NSCLC, has variants based on *EML4* breakpoints that affect fusion protein stability and response to ALK inhibitors [7–10].

*ROS1* fusions involve over 20 fusion partners and multiple breakpoints across introns 15–35, unlike *ALK* rearrangements which have a consistent breakpoint at intron 19 [2,11–14]. *CD74*, *EZR*, *SDC4*,

Abbreviations: NSCLC, non-small cell lung cancer; TKIs, tyrosine kinase inhibitors; DNA-NGS, DNA-based next generation sequencing; RT-PCR, reverse transcription-polymerase chain reaction; RNA-Seq, RNA sequencing; PFSR, progression-free survival rates; IHC, immunohistochemistry; FFPE, formalin-fixed paraffin-embedded; PD, progressive disease; CNVs, copy number variations; PR, partial response; TMD, transmembrane domain; PFR, progression-free survival.

\* Correspondence to: Department of Pathology, Asan Medical Center, University of Ulsan College of Medicine, 88, Olympic-ro 43-gil, Songpa-gu, Seoul 05505, Korea.

E-mail address: jenec@amc.seoul.kr (J. Choi).

https://doi.org/10.1016/j.ejca.2025.116091

Received 27 February 2025; Received in revised form 17 July 2025; Accepted 22 October 2025 Available online 2 November 2025

<sup>&</sup>lt;sup>c</sup> Astbury Centre for Structural Molecular Biology, Faculty of Biological Sciences, University of Leeds, Leeds, UK

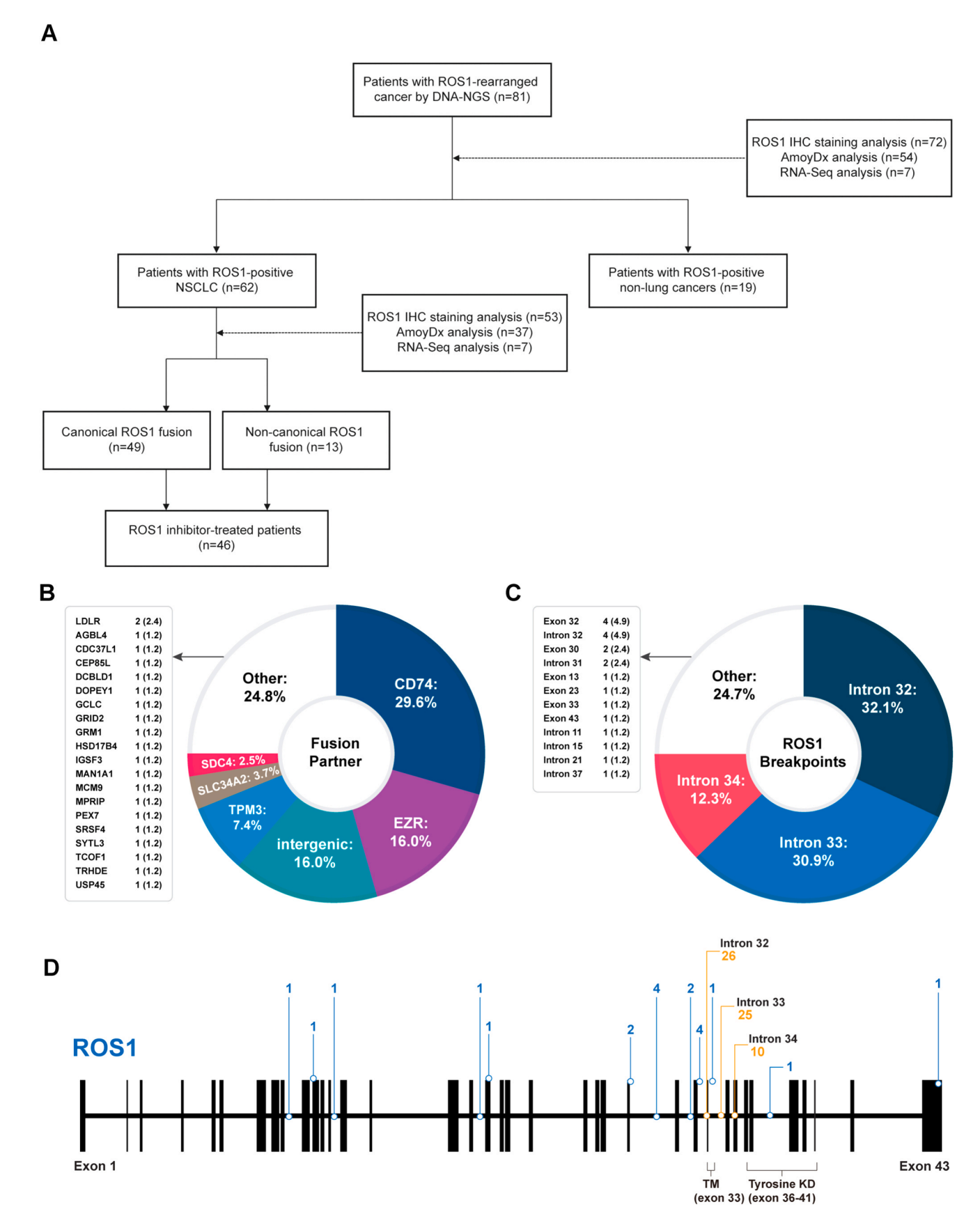


**Fig. 1.** Distribution of fusion partners and *ROS1* breakpoints among the entire study cohort of *ROS1* fusion-positive cancers. (A) Flow chart of patient selection and analysis. (B) Pie chart illustrating the frequency distribution of fusion partners. (C) Pie chart showing the distribution of *ROS1* breakpoint locations. (D) Schematic representation of the *ROS1* gene structure showing the distribution of breakpoints. Major *ROS1* breakpoints (introns 32, 33, and 34) are highlighted in orange. DNA-NGS, DNA based next generation sequencing; IHC, immunohistochemistry; RNA-Seq, RNA sequencing; NSCLC, non-small cell lung carcinoma.

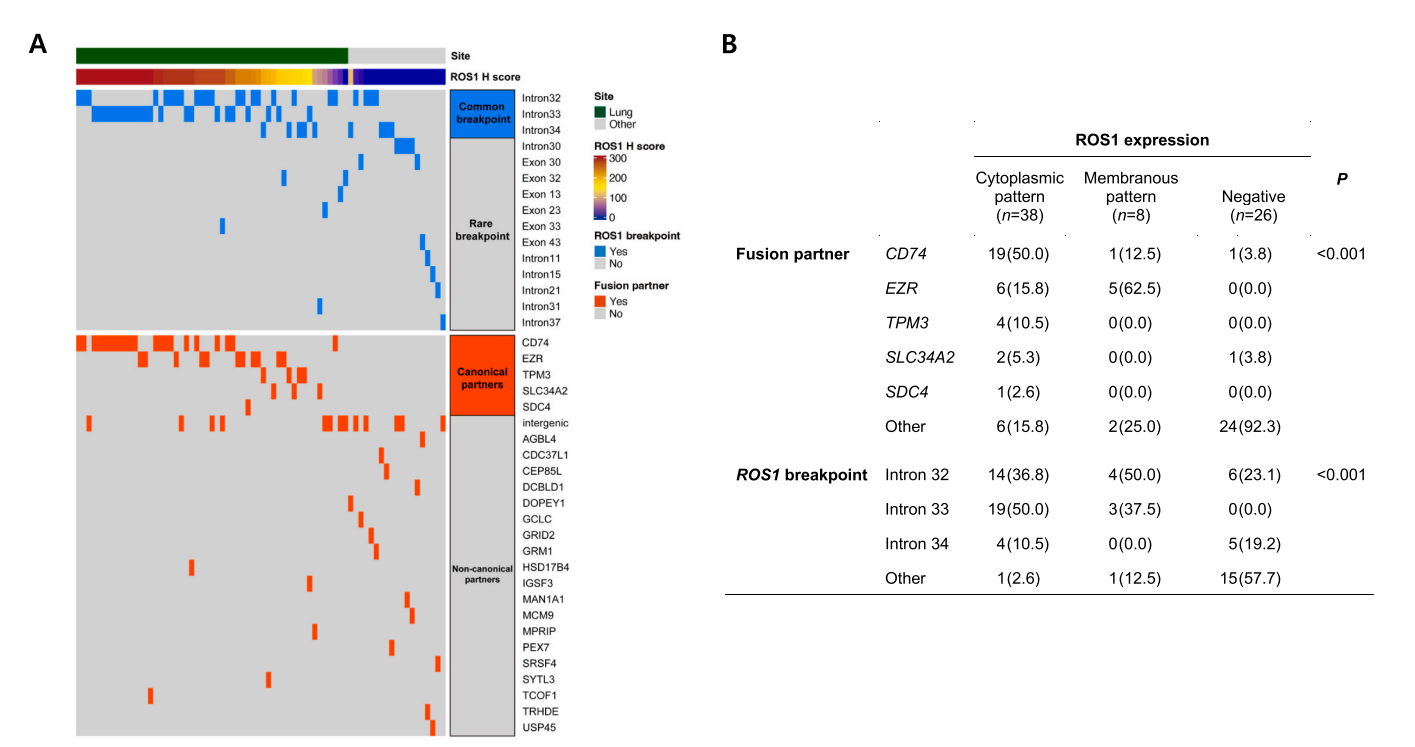


**Fig. 2.** Association of *ROS1* fusion variants with ROS1 expression. (A) Visualization of *ROS1* breakpoints, fusion partners, and ROS1 H-score distribution across the study cohort. Each column represents an individual case. The top bar indicates the primary tumor site (lung or other sites). H-scores are represented by a color gradient from blue (0) to red (300). *ROS1* breakpoints and fusion partners are indicated as present (blue or orange) or absent (gray) for each case. Breakpoint locations and fusion partners corresponding to each row are displayed on the left with their respective classification groups. (B) Distribution of *ROS1* breakpoints and fusion partners across ROS1 IHC staining patterns. ROS1 expression is significantly associated with both major *ROS1* breakpoints and canonical fusion partners (P < 0.001). Additionally, a membranous staining pattern is significantly associated with cases harboring an *EZR-ROS1* fusion.

Fusion partner	ROS1 breakpoints	n	DNA-NGS	RNA-Seq	В	Human (GRCh37/h)	p251 p25 p222 p21.	0 che6:117,645,341-117,64	5,816 Co 🗂 4 > 🕸	61 422 6232 633 434	2 925.2 926
CD74 (E6)	Intron 32	8	Out-frame	CD74(E6)-ROS1(E34)			117,645,400 hp	117,645,600 bp	476 bp	117,545,790 by	117,645,1
CD74 (E6)	Intron 33	12	In-frame	CD74(E6)-ROS1(E34)							
CD74 (E7)	Intron 33	3	In-frame	-				'		' '	
CD74 (within E7)	Intron 32	1	Undetermined	-							
EZR (E10)	Intron 32	7	Out-frame	<del>-</del>		Aligned sorted bem			-		
EZR (E10)	Intron 33	4	In-frame	EZR(E10)-ROS1(E34)						, ,	,
TPM3 (E8)	Intron 34	1	In-frame	-				anne: ROSI	Refseq Genes		
TPM3 (E10)	Intron 34	4	Out-frame	TPM3(E8)-ROS1(E35)				lecation chef 1176085 id: NM_002944.3 Exon number: 34 Amino acid coding num			
SLC34A2 (E13)	Intron 32	2	Out-frame	SLC34A2(E13)-ROS1(E34)		Sequence Ration Genes		clu6:117645495-117645	Ser 1865 578 h.gov/gene/honn-354_002944.3		
SDC4 (E4)	Intron 33	1	In-frame	-		tracks leaded	B (A+0.117.640.548				32984 of 4
				_							
DNA-NGS			•	RNA-Seq			Intron 6			Intron 32	
CD74-ROS1 (Intron 6-Intron 32)			CD74-ROS1 (Exon 6-Exon 34)			CD74 Exon	1-6 CD74	Exon 7–9	ROS1 Exon	1–32 ROS	1 Exon :
CD74-ROS1 (Intron 6-Intron 32)			CD74-ROS1 (Exon 6-Exon 34)				. /			/ .	
CD74-ROS1 (Intron 6-Intron 33)			CD74-ROS1 (Exon 6-Exon 34)								
SLC34A2-ROS1 (Exon 13-Intron 32)			SLC34A2-ROS1 (Exon13-Exon 34)			DNA	CD74 E	xon 1–6	ROS1 Exo	n 33–43	
EZR-ROS1 (Intron 10-Intron 33)			EZR-RO	EZR-ROS1 (Exon 10-Exon 34)					0		
TPM3-ROS1 (Exon 10-Intron 34)			TPM3-R	TPM3-ROS1 (Exon 8-Exon 35)				<b>↓</b>	ROS1	Exon 33	
Intergenic-ROS1 (chr12:32800653-Exon 33)			) CD74-R	OS1 (Exon 6-Exon 34)		RNA	CD74	Exon 1–6	ROS1 Exon 34	4_43	

Fig. 3. Comparison of *ROS1* fusion detection by DNA-NGS and RNA-Seq. (A) Detailed comparison of ROS1 fusion characteristics detected by DNA-NGS versus RNA-Seq. The table shows predicted fusion reading frames from DNA-NGS analysis and corresponding fusion transcripts identified by RNA-Seq validation. (B) Representative Integrative Genomics Viewer (IGV) image and schematic diagram from RNA-Seq analysis illustrating a *CD74-ROS1* fusion with a breakpoint in intron 32; exon 33 is excluded in the resulting fusion transcript to generate an in-frame fusion protein. (C) Comparative analysis of fusion transcripts identified by DNA-NGS and RNA-Seq, demonstrating the relationship between genomic breakpoint locations and the structure of the corresponding fusion transcripts. DNA-NGS, DNA-based next-generation sequencing; RNA-Seq, RNA sequencing; E, exon.

Table 1
Clinicopathologic characteristics of 62 NSCLC patients with ROS1 fusions.

Parameters		Patients (n, %	%)
		62	
Age (mean±sd)		59.44	(11.29)
Gender	Male	27	(43.5)
	Female	35	(56.5)
Diagnosis	ADC	58	(93.5)
	NSCLC	1	(1.6)
	SQCC	3	(4.8)
Smoking	Never smoker	38	(61.3)
	Ex-smoker	11	(17.7)
	Current	13	(21.0)
Stage	1	9	(14.5)
	2	7	(11.3)
	3	16	(25.8)
	4	30	(48.4)
Brain metastasis	Absent	52	(83.9)
	Present	10	(16.1)
ROS1 TKI	Yes	46	(74.2)
	No	16	(25.8)
Treatment	First line	14	(30.4)
	≥ Second line	32	(69.6)
Best response of	CR	2	(4.4)
of ROS1 TKI	PR	29	(64.4)
	SD	13	(28.9)
	PD	1	(2.2)
TMB (mean±SD)		11.17	(6.44)
AmoyDx		37	
	Positive	29	(78.4)
	Negative	8	(21.6)
ROS1 IHC		53	
	Positive	46	(86.8)
	Negative	7	(13.2)
ROS1H score (mean (sd))		233.30	(86.11)

sd: standard deviation; ADC: adenocarcinoma; SQCC: squamous cell carcinoma; TKI: tyrosine kinase inhibitor; CR: complete response; PR: partial response; SD: stable disease; PD: progressive disease; TMB: tumor mutational burden; IHC: immunohistochemistry.

*SLC34A2*, and *TPM3* are classified as canonical fusion partners, with introns 31–35 being common breakpoints in NSCLCs [2,7,15]. While *ROS1* fusion variants have been analyzed based on both fusion partners and breakpoints, previous studies investigating therapeutic responses and prognoses in NSCLCs have focused predominantly on fusion partners, with conflicting results [12,16–20].

We conducted a comprehensive analysis of *ROS1*-rearranged cancers using targeted DNA next-generation sequencing (DNA-NGS), reverse transcription polymerase chain reaction (RT-PCR), RNA sequencing (RNA-Seq), and immunohistochemistry (IHC), and evaluated the correlation between *ROS1*-fusion variants and response to ROS1 inhibitors in ROS1-positive NSCLCs.

## 2. Materials and methods

Detailed descriptions of clinical, molecular, and analytical methods are provided in Supplementary Materials and Methods.

# 2.1. Patients

We analyzed 81 *ROS1* fusion-positive cases identified through DNA-NGS testing (AMC OncoPanel v4.0) between 2009 and 2021 at Asan Medical Center. Clinical data including demographics, pathologic findings, and survival data were reviewed. The study protocol was approved by the Institutional Review Board of Asan Medical Center (IRB No.2022–1595).

# 2.2. NGS analysis

DNA-NGS was performed using FFPE tumor tissues on the HiSeq

platform with OncoPanel AMC version 4.0, detecting mutations in 323 genes, as previously described [21]. RNA-Seq was conducted using from FFPE tissues on an Illumina NovaSeq (Illumina, Inc., San Diego, CA) by Macrogen Incorporated (Seoul, Korea) to confirm fusion transcripts. Fusion transcripts were identified using STAR-Fusion (v1.12.0) within the Trinity Cancer Transcriptome Analysis Toolkit framework [22,23].

#### 2.3. Immunohistochemistry

ROS1 expression was assessed in 72 cases using SP384 clone on the Ventana BenchMark XT. Staining intensity was scored as strong (3+), moderate (2+), weak (1+), or negative (0), with H-score cutoff  $\geq$  150 (Supplementary Fig 1) [24].

#### 2.4. AmoyDx

RT-PCR assay was performed to confirm canonical *ROS1* fusions, detecting 14 common fusion types [25,26].

## 3. Results

#### 3.1. Clinicopathologic features of the patient cohorts

DNA-NGS was used to analyze the 81 patients harboring *ROS1* fusions included in the present study cohort (Supplementary Table 1). The predominant primary tumor site was the lung (76.5 %), followed by the brain and stomach (6.2 %), and the prostate and soft tissue (2.5 %). AmoyDx was used in 54 cases (66.6 %), yielding 30 positive (55.6 %) and 24 negative (44.4 %) results. ROS1 IHC was conducted for 72 cases (88.9 %), resulting in 46 positive (63.9 %) and 26 negative (36.1 %) findings (Fig. 1A).

## 3.2. Heterogeneity of ROS1 fusion and variable ROS1 expression

Based on the DNA-NGS data, a diverse distribution of *ROS1* breakpoints and *ROS1* fusion partners was evident among the study patients. Among 48 canonical fusions [2,15,16], *CD74* was the most prevalent fusion partner (29.6 %), followed by *EZR* (16.0 %), *TPM3* (7.4 %), *SLC34A2* (3.7 %), and *SDC4* (2.5 %). The remaining 33 cases were either non-canonical rare fusions (24.7 %) or intergenic-*ROS1* fusions (16.0 %) (Fig. 1B).

Regarding *ROS1* breakpoints, intron 32 was the most common (32.1 %), followed by intron 33 (30.9 %), and intron 34 (12.3 %). The remaining 20 cases (24.7 %) comprised a diverse range of uncommon breakpoints, spanning from intron 11 to exon 43. In this cohort, introns 32, 33, and 34 were classified as the major breakpoint regions in *ROS1* (Fig. 1C, D).

IHC analysis of 72 cases (89 %) revealed strong associations between ROS1 expression levels and both ROS1 breakpoints and fusion partners (P < 0.001, Fig. 2A). High ROS1 expression correlated with major breakpoints of introns 32, 33, and 34, and canonical fusion partners, predominantly in NSCLCs. Low expression was associated with rare breakpoints and non-canonical partners, mainly in non-lung cancers. Membranous staining pattern showed strong correlation with *EZR-ROS1* fusion (P < 0.001, Fig. 2B).

In the NSCLC subset (n = 62), the distribution of fusion partners and *ROS1* breakpoints were similar to the entire cohort, with *CD74* remaining the predominant partner (38.7 %) and major breakpoints occurring in introns 33 (40.3 %), 32 (35.5 %), and 34 (9.7 %) (Supplementary Fig. 2). ROS1 expression levels significantly correlated with both breakpoint location (P = 0.002) and fusion partners (P = 0.010, Supplementary Table 2).

# 3.3. Molecular characteristics of ROS1 fusion variants

We analyzed the in-frame status of ROS1 fusions detected by DNA-

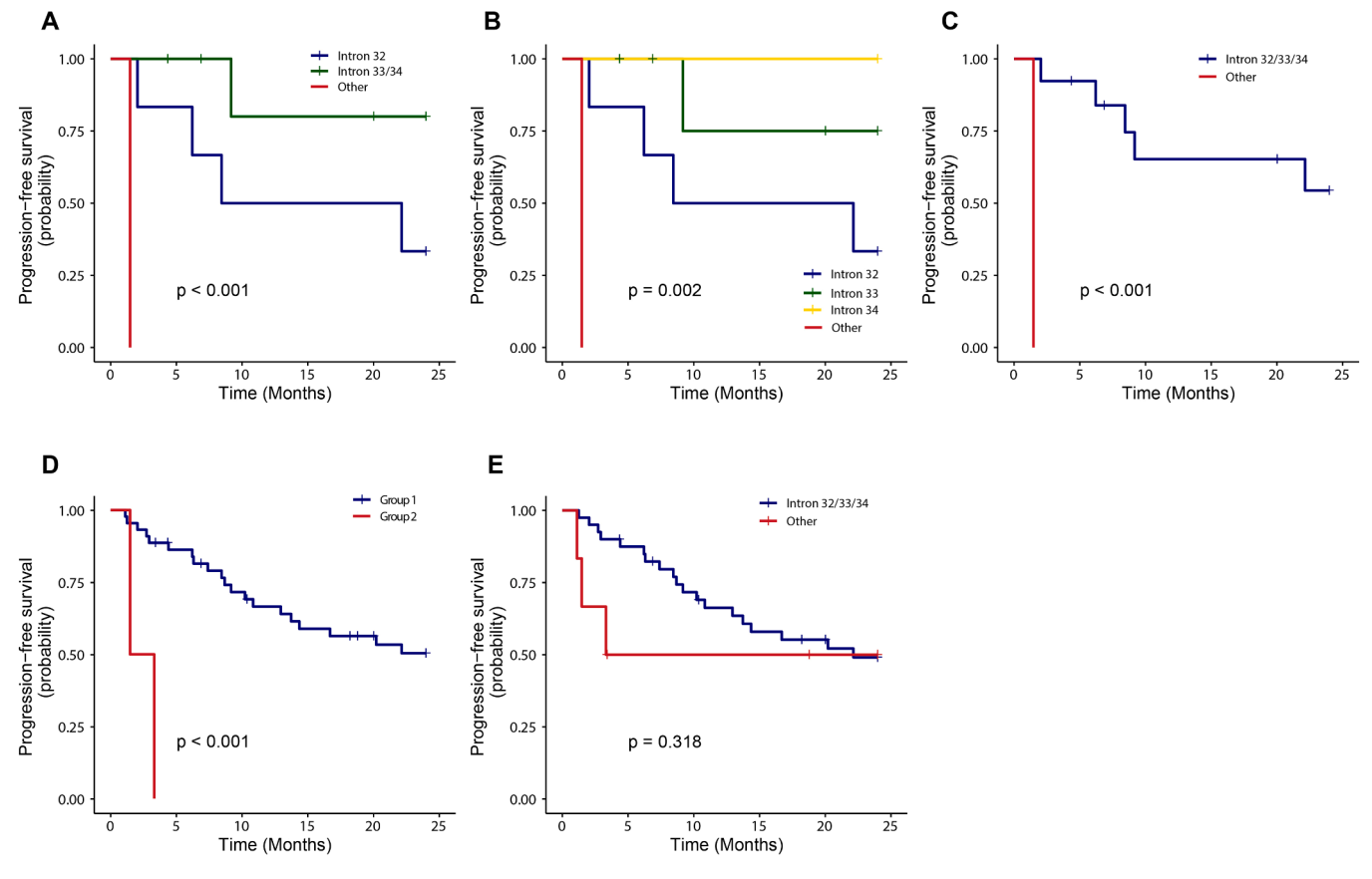


Fig. 4. Progression-free survival analysis using Kaplan-Meier curves of *ROS1*-rearranged NSCLC patients treated with ROS1-TKIs based on *ROS1* fusion variants. (A) PFS comparison among patients with *ROS1* breakpoints in intron 32, introns 33/34, and other regions among the first-line TKI-treated patients. (B) Detailed PFS analysis of first-line TKI-treated patients with breakpoints in introns 32, 33, 34, and other regions. (C) PFS comparison between patients with major breakpoints (introns 32/33/34) and other breakpoints among first-line TKI-treated patients. (D) PFS comparison between Group 1 patients (with either major breakpoints or canonical fusion partners) and Group 2 patients (with both rare breakpoints and non-canonical fusion partners) among all of the TKI-treated patients. (E) PFS comparison between patients with major breakpoints (introns 32/33/34) and other breakpoints among all TKI-treated patients.

NGS, finding that canonical fusion partners had various breakpoints (Fig. 3A). Notably, *ROS1* breakpoints in intron 32 generated potential out-of-frame fusions regardless of fusion partners. RNA-Seq analysis of seven cases revealed that fusion transcripts with intron 32 breakpoints exclude exon 33 and start from exon 34 to produce in-frame transcripts (Fig. 3B&C). Although RNA-Seq was not performed in all cases with a breakpoint in intron 32 due to an insufficient availability of tumor tissues, these data suggested that the fusions with an *ROS1* breakpoint in intron 32 are likely excluding exon 33 (which encodes the transmembrane domain of ROS1) at the transcript level and that this could be equivalent to cases with an *ROS1* breakpoint in intron 33.

Most cases with canonical fusion partners (38/40, 95 %) exhibited ROS1 expression (Fig. 2B), with significant partner preference for ROS1 breakpoints; notably, *CD74* preferentially fused with intron 33 (P < 0.001) (Supplementary Table 3). In addition, among 13 cases with intergenic-ROS1 fusion, four cases were reclassified by AmoyDx as canonical fusions with ROS1 IHC positivity (mean H score: 290.0 [ $\pm$  8.17], Supplementary Table 4) and one case was switched to a canonical *CD74-ROS1* fusion by RNA-Seq. Moreover, one out-of-frame fusion of *TPM3-ROS1* with a breakpoint in *TPM3* exon 10 were corrected to a breakpoint in *TPM3* intron 8 by RNA-Seq (Fig. 3C). These results suggested that *ROS1* breakpoints are an important factor in the creation of in-frame fused proteins.

# 3.4. Treatment response in NSCLCs patients with different ROS1 fusion variants

Among the 81 study patients with *ROS1* fusion cancers, 62 NSCLC cases (76.5%) were further analyzed (Table 1 and Fig. 1A). Most of these NSCLC patients had been diagnosed with adenocarcinoma (93.5%) and had advanced-stage disease (stage III and IV, 74.2%). AmoyDx and subsequent RNA-Seq analyses stratified these cases into 49 canonical and 13 non-canonical fusions. ROS1-TKIs, including crizotinib, ceritinib, loratinib, and repotrectinib, had been administered to 46 of the study patients (74.2%), with 14 receiving it as first-line therapy and 32 as second-line or later treatment.

Among the ROS1-TKI treated NSCLC patients, the 2-year progression-free survival rate (PFSR) was 48.2% (95 % CI: 35.1–66.2), with a median PFS (mPFS) of 22.1 months (95 % CI: 12.9–NA). For first-line treatment, the PFSR was 50.5% (CI: 28.4–89.8), with mPFS not reached (CI: 8.4–NA). A significantly lower PFSR was observed in patients with ROS1 breakpoints in intron 32 and other regions compared to introns 33 and 34 (intron 32, 33.3% [CI: 10.8–100]; introns 33 and 34, 80% [CI: 51.6–100]; other, 9% [CI: NA–NA], 90.001, Fig. 90

The 46 ROS1-TKI treated NSCLC patients were subclassified into two groups: Group 1 (major *ROS1* breakpoints or canonical fusion partners) and Group 2 (rare partners and non-major breakpoints). Group 2 had a significantly lower PFSR (Group 2, 0 % [CI: NA–NA]; Group 1, 50.4 %

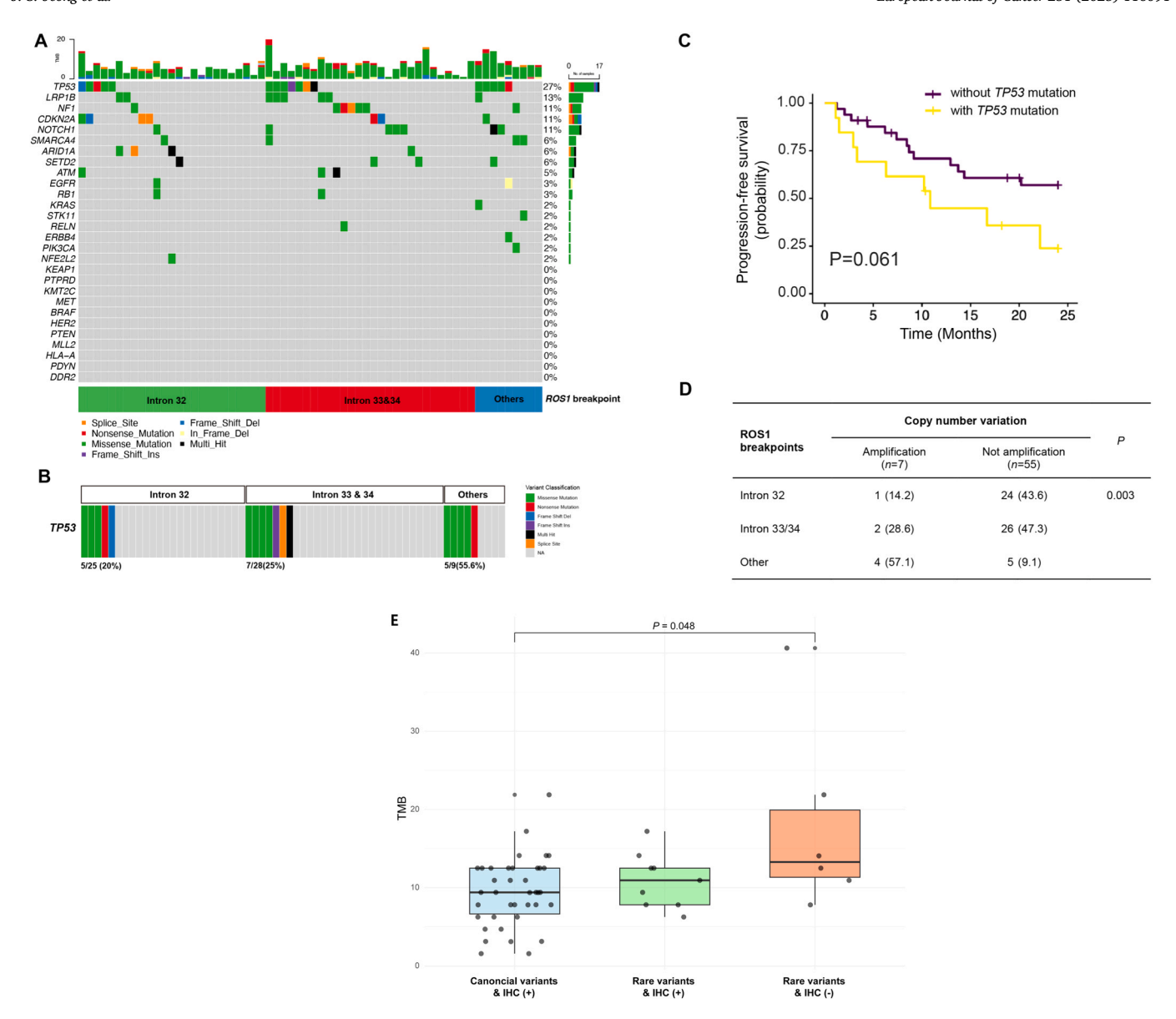


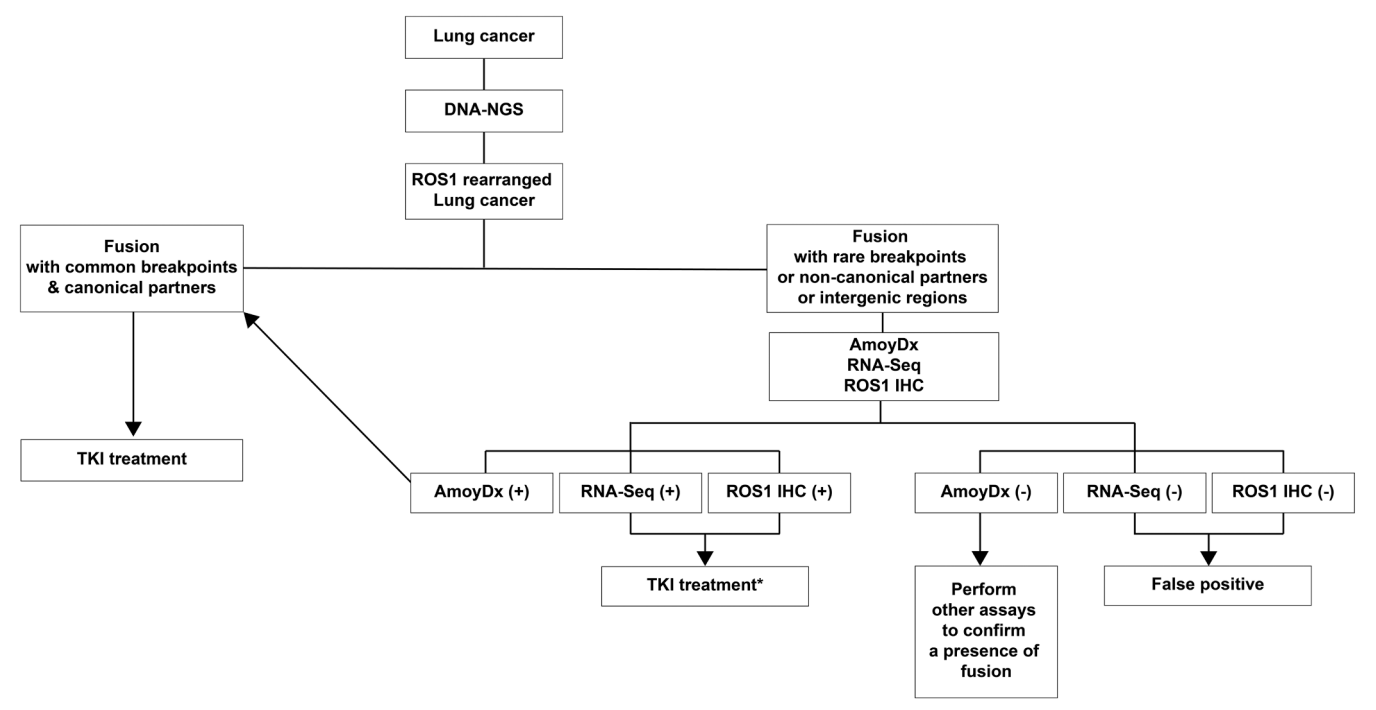
**Fig. 5.** Genomic landscape and therapeutic effects in *ROS1* fusion-positive NSCLC patients with *ROS1* breakpoints. (A) Oncoprint visualization of the genomic alterations associated with different *ROS1* breakpoints. (B) Distribution of *TP53* mutations across different *ROS1* breakpoint locations. (C) Kaplan-Meier curves of PFS outcomes in patients stratified by the presence or absence of *TP53* mutations. (D) Association between copy number variations and *ROS1* breakpoints. (E) A comparative analysis of tumor mutation burden (TMB). Canonical variants include major *ROS1* breakpoints and canonical fusion partners, while rare variants include uncommon ROS1 breakpoints and non-canonical fusion partners. IHC, immunohistochemistry.

[CI: 36.9–68.8], P < 0.001, Fig. 4D). When patients were categorized by major common versus rare *ROS1* breakpoints, those with rare *ROS1* breakpoints tended to have lower PFSR (other, 50 % [CI: 22.5–1]; introns 32/33/34, 49.1 % [CI: 35.2–68.4], P = 0.318, Fig. 4E).

In univariable analysis the comparison between Group 1 and Group 2 was the only factor found to be statistically associated with the PFS (HR 12.1, CI 2.3–63.5, P=0.003) (Supplementary Table 5). We further analyzed patients with uncommon breakpoints of *ROS1* and received TKI treatment in accordance with the ROS1 expression profile. Among the five patients with uncommon *ROS1* breakpoints who received TKI treatment, two showed ROS1 IHC positivity and achieved a partial response (PR) as their best response. In contrast, patients with ROS1 IHC negativity had a lower PFSR (0 % [CI: NA–NA] vs. 50 % [CI: 12.5–100 %], P=0.063; see Supplementary Fig. 3).

# 3.5. Comparing concomitant genetic alteration with ROS1 breakpoints

We analyzed concomitant genetic alterations in terms of ROS1 breakpoints, focusing on genes known to harbor major mutations in NSCLCs [27]. The TP53 mutations were found in these analyses to the most common concomitant mutations in the ROS1-rearranged lung cancers, followed by LRP1B, NF1, and CDKN2A (Fig. 5A). Specifically, among cases with TP53 mutations, 22.7 % had breakpoints in intron 32, 22.6 % in intron 33 and 34, and 55.6 % in other regions. Thus, TP53 mutations were more frequent in cases with other region breakpoints compared to major ROS1 breakpoints (P=0.113, Fig. 5B). In addition, patients with a TP53 mutation showed a tendency toward a poorer PFS compared with TP53 wild-type cases (P=0.061, Fig. 5C) regardless of the status of the ROS1 fusion partner and breakpoint. The CNVs of key genes in NSCLCs, including EGFR, ERBB2, ET, ET, ET, ET, ET, and ET, ET, were also further analyzed (Supplementary Table 6), and revealed that the CNVs of oncogenes were more frequent in cases with rare



\* Patients with lung cancer harboring ROS1 fusions with breakpoints in intron 32 or non-canonical fusion partners may have poor prognosis with TKI treatment.

**Fig. 6.** Validation algorithm for *ROS1* fusions detected by DNA-NGS. Fusions with common partners and breakpoints may proceed directly to treatment, while those with uncommon variants require additional validation using AmoyDx, RNA-Seq, or immunohistochemistry (IHC). DNA-NGS, DNA based next generation sequencing; IHC, immunohistochemistry; RNA-Seq, RNA sequencing.

breakpoints than in those with major breakpoints of *ROS1* (P = 0.003, Fig. 5D). In the comparison of tumor mutation burden (TMB), cases with rare fusion variants and negative ROS1 IHC showed significantly higher TMB than those with canonical fusion variants. (P = 0.048; Fig. 5E).

## 4. Discussion

We found that an *ROS1* breakpoint is an important response factor for ROS inhibitors. *ROS1* fusions with rare or intron 32 breakpoints showed strong associations with non-canonical fusion partners, reduced ROS1 expression, and poor clinical outcomes. Our findings thus suggest that a precise pinpointing of the fusion partner and breakpoint in *ROS1* fusions is more important than simply detecting the *ROS1* rearrangement when stratifying patients who are likely to respond to ROS-TKIs.

We analyzed 81 *ROS1*-rearranged cases using comprehensive analysis. Among these, 20 cases (24.7 %) had rare fusion partners, and 13 (16.0 %) harbored intergenic-*ROS1* fusions. Fourteen NSCLC cases initially classified as non-canonical or intergenic *ROS1* fusions were reclassified by AmoyDx with strong ROS1 expression (mean H-score: 290.0). The remaining eight NSCLC cases had low ROS1 expression (mean H-score: 106.3), with four patients receiving ROS1 TKI treatments: three achieving PR and one experiencing PD, all eventually progressing (Supplementary Table 7). Non-NSCLC cases with negative AmoyDx findings exhibited no ROS1 expression (mean H-score: 6.9), suggesting a cautious interpretation of rare *ROS1* fusions due to the limitations of DNA-NGS. We further found that rare fusion partners mainly exhibited ROS1 IHC negativity, and combining DNA-NGS with IHC may improve the detection of rare *ROS1* fusion-positive NSCLC cases (Fig. 2).

In diverse fusion *ROS1* fusion variants [12,15,17–19], Zhou et al. [3] reported that common fusions occur in introns 31–33 and uncommon fusions arise in introns 34 and 35. In our present cohort, we identified 12 minor exonic and intronic breakpoints and 3 major breakpoints (introns 32–34) by DNA-NGS. Canonical fusion partners were usually associated with major breakpoints with high ROS1 expression, whereas

non-canonical partners tended to have rare *ROS1* breakpoints with low ROS1 expression (Fig. 2B). These findings suggest that canonical fusion partners tend to produce in-frame fusions, whereas cases with rare partners and minor breakpoints may not generate functional *ROS1* transcripts, potentially leading to varied responses to ROS1-TKIs.

We next found that breakpoints in intron 32 makes potential out-of-frame fusions with canonical fusion partners. For example, the *EZR-ROS1* fusion, typically breaking at intron 10: intron 32 [3], is an out-of-frame fusion at genomic level (Fig. 3). RNA-Seq revealed that in cases harboring a *ROS1* intron 32 break, exon 33 had been excluded, producing equivocal transcripts to those with breakpoints in intron 33, potentially to generate a functional transcript. Thus, *ROS1* breakpoints at genomic levels do not always match actual fusion transcripts.

We additionally noted that exon 33 encodes the single transmembrane domain (TMD) of ROS1. Although RNA-Seq was not performed for all cases with intron 32 breaks, most canonical fusions with an intron 32 breakpoint may exclude the ROS1 TMD from the final protein product, similar to those with breakpoints at introns 33 and 34. These findings explain the cytoplasmic staining pattern of ROS1 in most ROS1 fusion-positive cancers except for EZR-ROS1 fusions (Fig. 2B) [28, 29]. The most interesting aspect of the TMD of *ROS1* is whether it affects the clinical responses to ROS1-TKIs. Li and colleagues have reported previously that CD74-ROS1 fusions with the TMD (long ROS1-fusion group) show poorer responses to crizotinib than CD74-ROS1 fusions without the TMD (short ROS1-fusion group) [16]. Overall, we speculate that the post-transcriptional process for excluding exon 33 to create an in-frame transcript might not always be complete. Several types of CD74-ROS1 fusions could therefore occur, leading to differences in the PFSR between long and short ROS1-fusion groups and resulting in poorer outcomes for CD74-ROS1 fusions [17,19]. However, we found no outcome differences between patients with CD74-ROS1 fusions and those with non-CD74-ROS1 fusions (Supplementary Fig. 4).

Among ROS1-rearranged NSCLC patients in the cohort, those with intron 33/34 rearrangements had significantly longer PFS than those with intron 32 rearrangements (P < 0.001, Fig. 4A, B). Patients with

rare partners and non-major breakpoints showed a poorer PFS outcome (P < 0.001, Fig. 4D). These findings suggested that actual in-frame functional fusions may be a crucial factor for ROS1-TKI responses. Thus, canonical fusion partners and breakpoints in introns 33 and 34 may represent the optimal combination for effective ROS1-TKI therapy and ROS1 fusions involving uncommon partners or rare breakpoints require further evaluation. In this context, patient stratification and prediction of clinical response to next-generation ROS1-TKIs remain challenging. We provide a simplified summary of an optimized diagnostic approach to identify ROS1-positive patients most likely to benefit from ROS1-targeted therapy, accounting for the limitations of current testing platforms (Fig. 6).

Previous studies have reported that *ROS1* fusion-positive tumors generally harbor fewer driver mutations and genomic alterations [30]. In contrast, we observed a significantly higher prevalence of CNVs, higher TMB, and a tendency toward more frequent *TP53* mutation in cases with rare *ROS1* breakpoints. We hypothesize that these cases may not have functional ROS1 fusion products. Notably in this regard, all three in our study population with uncommon breakpoints showed ROS1 IHC negativity and PD during TKI treatment (Supplementary Fig. 3).

In conclusion, for the first time to our knowledge, we have observed an association between major and minor *ROS1* breakpoints, fusion partners, and the ROS1-TKI response in *ROS1*-rearranged cancers and that not all canonical fusion partners produce functional fusion products. Canonical fusion partners with introns 33 and 34 of *ROS1* could be the predictors of the patients likely to have the most optimal ROS1-TKI benefit. Hence, other rare *ROS1* fusions identified by DNA-NGS should be further assessed to pinpoint the specific fusion partners and *ROS1* breakpoints.

## CRediT authorship contribution statement

Josephina Sampson: Software, Formal analysis. Deokhoon Kim: Investigation, Data curation. Shinkyo Yoon: Methodology, Data curation. Yeokyeong Shin: Methodology, Data curation. Jeong Ji Seon: Writing – original draft, Visualization, Methodology, Investigation, Formal analysis, Data curation. Jene Choi: Writing – review & editing, Supervision, Funding acquisition, Conceptualization. Richard Bayliss: Investigation, Formal analysis.

## **Funding**

This work was supported by the National Research Foundation of Korea (NRF) grant (No. 2020R1A2C2006815) funded by the Korean government (MSIT).

# **Declaration of Competing Interest**

The authors declare that they have no known competing financial interests or personal relationships that could have appeared to influence the work reported in this paper.

# Acknowledgements

Not applicable.

## Appendix A. Supporting information

Supplementary data associated with this article can be found in the online version at doi:10.1016/j.ejca.2025.116091.

#### References

- [1] Kohno T, Nakaoku T, Tsuta K, Tsuchihara K, Matsumoto S, Yoh K, et al. Beyond ALK-RET, ROS1 and other oncogene fusions in lung cancer. Transl Lung Cancer Res 2014;4:156–64. https://doi.org/10.3978/j.issn.2218-6751.2014.11.11.
- [2] Drilon A, Jenkins C, Iyer S, Schoenfeld A, Keddy C, Davare MA. ROS1-dependent cancers — biology, diagnostics and therapeutics. Nat Rev Clin Oncol 2021;18: 35–55. https://doi.org/10.1038/s41571-020-0408-9.
- [3] Zhou S, Zhang F, Xu M, Zhang L, Liu Z, Yang Q, et al. Novel insights into molecular patterns of ROS1 fusions in a large Chinese NSCLC cohort: a multicenter study. Mol Oncol 2023;17:2200–12. https://doi.org/10.1002/1878-0261.13509.
- [4] Kim HH, Lee JC, Oh I-J, Kim EY, Yoon SH, Lee SY, et al. Real-world outcomes of crizotinib in ROS1-rearranged advanced non-small-cell lung cancer. Cancers 2024; 16:528. https://doi.org/10.3390/cancers16030528.
- [5] Shaw AT, Riely GJ, Bang Y-J, Kim D-W, Camidge DR, Solomon BJ, et al. Crizotinib in ROS1-rearranged advanced non-small-cell lung cancer (NSCLC): updated results, including overall survival, from PROFILE 1001. Ann Oncol 2019;30:1121–6. https://doi.org/10.1093/annonc/mdz131.
- [6] Wu Y-L, Yang JC-H, Kim D-W, Lu S, Zhou J, Seto T, et al. Phase II study of crizotinib in east asian patients with ROS1-positive advanced non-small-cell lung cancer. J Clin Oncol 2018;36:1405–11. https://doi.org/10.1200/jco.2017.75.5587.
- [7] Woo CG, Seo S, Kim SW, Jang SJ, Park KS, Song JY, et al. Differential protein stability and clinical responses of EML4-ALK fusion variants to various ALK inhibitors in advanced ALK-rearranged non-small cell lung cancer. Ann Oncol 2017; 28:791–7. https://doi.org/10.1093/annonc/mdw693.
- [8] Su Y, Long X, Song Y, Chen P, Li S, Yang H, et al. Distribution of ALK fusion variants and correlation with clinical outcomes in chinese patients with non-small cell lung cancer treated with crizotinib. Target Oncol 2019;14:159–68. https://doi. org/10.1007/s11523-019-00631-x.
- [9] Wang S, Luo R, Shi Y, Han X. The impact of the ALK fusion variant on clinical outcomes in EML4-ALK patients with NSCLC: a systematic review and metaanalysis. Futur Oncol 2021;18:385–402. https://doi.org/10.2217/fon-2021-0945.
- [10] Li Y, Zhang T, Zhang J, Li W, Yuan P, Xing P, et al. Response to crizotinib in advanced ALK-rearranged non-small cell lung cancers with different ALK-fusion variants. Lung Cancer 2018;118:128–33. https://doi.org/10.1016/j. lungcan.2018.01.026.
- [11] Ou S-HI, Nagasaka M. A Catalog of 5' fusion partners in ROS1-positive NSCLC Circa 2020. JTO Clin Res Rep 2020;1:100048. https://doi.org/10.1016/j. itocrr 2020 100048
- [12] Cui M, Han Y, Li P, Zhang J, Ou Q, Tong X, et al. Molecular and clinicopathological characteristics of ROS1-rearranged non-small-cell lung cancers identified by nextgeneration sequencing. Mol Oncol 2020;14:2787–95. https://doi.org/10.1002/ 1878-0261.12789.
- [13] Nagasaka M, Zhang SS, Baca Y, Xiu J, Nieva J, Vanderwalde A, et al. Pan-tumor survey of ROS1 fusions detected by next-generation RNA and whole transcriptome sequencing. BMC Cancer 2023;23:1000. https://doi.org/10.1186/s12885-023-11457-2.
- [14] Ou S-HI, Zhu VW, Nagasaka M. Catalog of 5' fusion partners in ALK-positive NSCLC Circa 2020. JTO Clin Res Rep 2020;1:100015. https://doi.org/10.1016/j jtocrr.2020.100015.
- [15] Li W, Guo L, Liu Y, Dong L, Yang L, Chen L, et al. Potential unreliability of uncommon ALK, ROS1, and RET genomic breakpoints in predicting the efficacy of targeted therapy in NSCLC. J Thorac Oncol 2021;16:404–18. https://doi.org/ 10.1016/j.jtho.2020.10.156.
- [16] Li W, Fei K, Guo L, Wang Y, Shu C, Wang J, et al. CD74/SLC34A2-ROS1 fusion variants involving the transmembrane region predict poor response to crizotinib in NSCLC independent of TP53 mutations. J Thorac Oncol 2024;19:613–25. https:// doi.org/10.1016/j.jtho.2023.12.009.
- [17] Zhang Y, Zhang X, Zhang R, Xu Q, Yang H, Lizaso A, et al. Clinical and molecular factors that impact the efficacy of first-line crizotinib in ROS1-rearranged nonsmall-cell lung cancer: a large multicenter retrospective study. BMC Med 2021;19: 206. https://doi.org/10.1186/s12916-021-02082-6.
- [18] He Y, Sheng W, Hu W, Lin J, Liu J, Yu B, et al. Different types of ROS1 fusion partners yield comparable efficacy to crizotinib. Oncol Res 2019;27:901–10. https://doi.org/10.3777/096504019v15509372008132
- [19] Li Z, Shen L, Ding D, Huang J, Zhang J, Chen Z, et al. Efficacy of crizotinib among different types of ROS1 fusion partners in patients with ROS1-rearranged non-small cell lung cancer. J Thorac Oncol 2018;13:987–95. https://doi.org/ 10.1016/j.ithp.2018.04.016
- [20] Xu H, Zhang Q, Liang L, Li J, Liu Z, Li W, et al. Crizotinib vs platinum-based chemotherapy as first-line treatment for advanced non-small cell lung cancer with different ROS1 fusion variants. Cancer Med 2020;9:3328–36. https://doi.org/ 10.1002/cam4.2984.
- [21] Hwang HS, Kim D, Choi J. Distinct mutational profile and immune microenvironment in microsatellite-unstable and POLE-mutated tumors. J Immunother Cancer 2021;9:e002797. https://doi.org/10.1136/jitc-2021-002797
- [22] Haas BJ, Dobin A, Li B, Stransky N, Pochet N, Regev A. Accuracy assessment of fusion transcript detection via read-mapping and de novo fusion transcript assembly-based methods. Genome Biol 2019;20:213. https://doi.org/10.1186/ c12050.010.1842.0
- [23] Xu Y, Shi X, Wang W, Zhang L, Cheung S, Rudolph M, et al. Prevalence and clinico-genomic characteristics of patients with TRK fusion cancer in China. Npj Precis Oncol 2023;7:75. https://doi.org/10.1038/s41698-023-00427-3.
- [24] Conde E, Hernandez S, Martinez R, Angulo B, Castro JD, Collazo-Lorduy A, et al. Assessment of a New ROS1 Immunohistochemistry Clone (SP384) for the

- Identification of ROS1 Rearrangements in Patients with Non–Small Cell Lung Carcinoma: the ROSING Study. J Thorac Oncol 2019;14:2120–32. https://doi.org/10.1016/j.jtho.2019.07.005.
- [25] Co.} {Amoy Diagnostics. AmoyDx® ROS1Gene Fusions Detection Kit 2022.
- [26] Service HIR& A Reimbursement Criteria for Crizotinib 2019.
- [27] Suster DI, Mino-Kenudson M. Molecular pathology of primary non-small cell lung cancer. Arch MéD Res 2020;51:784–98. https://doi.org/10.1016/j. arcmed.2020.08.004.
- [28] Yoshida A, Tsuta K, Wakai S, Arai Y, Asamura H, Shibata T, et al. Immunohistochemical detection of ROS1 is useful for identifying ROS1
- rearrangements in lung cancers. Mod Pathol 2014;27:711–20. https://doi.org/10.1038/modpathol.2013.192.
- [29] Bruce B, Khanna G, Ren L, Landberg G, Jirström K, Powell C, et al. Expression of the cytoskeleton linker protein ezrin in human cancers. Clin Exp Metastas 2007;24: 69–78. https://doi.org/10.1007/s10585-006-9050-x.
- [30] Huang RSP, Haberberger J, Sokol E, Schrock AB, Danziger N, Madison R, et al. Clinicopathologic, genomic and protein expression characterization of 356 ROS1 fusion driven solid tumors cases. Int J Cancer 2021;148:1778–88. https://doi.org/ 10.1002/ijc.33447.